AD-A130 188 PLASMA THEORY AND SIMULATION(U) CALIFORNIA UNIV 1/1
BERKELEY ELECTRONICS RESEARCH LAB C K BIRDSALL
30 JUN 82 N00014-77-C-0578

UNCLASSIFIED F/G 20/9 NL

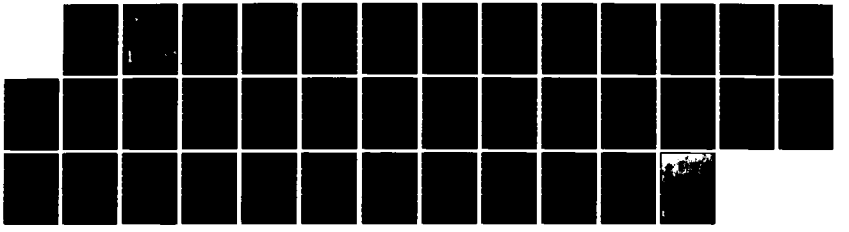

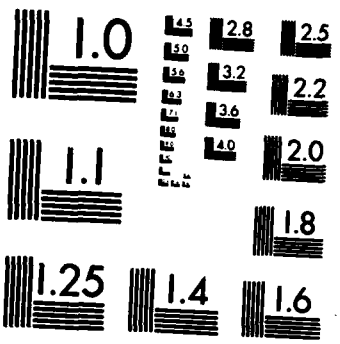

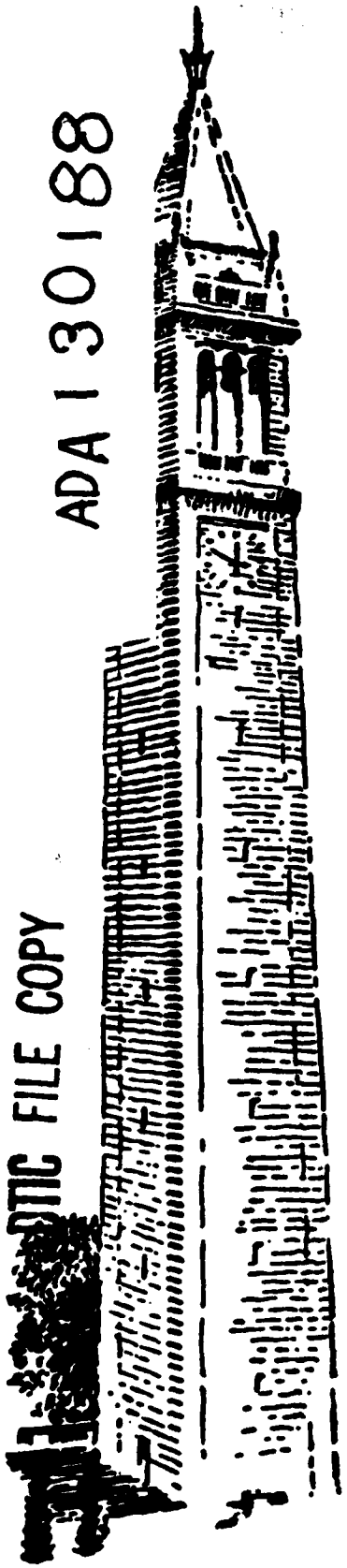

FIRST & SECOND QUARTER PROGRESS REPORT

ON

PLASMA THEORY AND SIMULATION

January 1 to June 30, 1982

DOE Contract DE-AT03-76ET53054
ONR Contract N00014-77-C-0578

ELECTRONICS RESEARCH LABORATORY
College of Engineering
University of California, Berkeley, CA 94720

FIRST & SECOND QUARTER PROGRESS REPORT
on
PLASMA THEORY AND SIMULATION

January 1 to June 30, 1982

Our research group uses both theory and simulation as tools in order to increase the understanding of instabilities, heating, transport, and other phenomena in plasmas. We also work on the improvement of simulation, both theoretically and practically.

Our staff is —

*Professor C.K. Birdsall**	*191M*	*Cory Hall*	*(642-4015)*
Principal Investigator			
Dr. Thomas L. Crystal	*119ME*	*Cory Hall*	*(642-3477)*
Post-Doctorate; Lecturer, UCB			
Dr. Bruce Cohen	*L630*	*LLNL*	*(422-9823)*
Dr. A. Bruce Langdon	*L477*	*LLNL*	*(422-5444)*
Dr. William Nevins	*L630*	*LLNL*	*(422-7032)*
Lecturers, UCB; Physicists LLNL			
Dr. Mary Hudson		*SSL*	*(642-1327)*
Guest, UCB; Senior Fellow, Space Science Lab.			
Mr. Kwang-Youl Kim			
Mr. William Lawson			
Mr. Niels Otani			
Mr. Stéphane Rousset			
Mr. Vincent Thomas	*119MD*	*Cory Hall*	*(642-1297)*
Research Assistants			

June 30, 1982

DOE Contract DE-AT03-76ET53064-DE-AM03-76SF00034
ONR Contract N00014-77-C-0578

ELECTRONICS RESEARCH LABORATORY

University of California
Berkeley, California 94720

* On sabbatical leave at Institute of Plasma Physics, Nagoya University, Nagoya 464, Japan until Feb 28, 1982 (host T. Kamimura); on leave at California Institute of Technology, Pasadena CA 91125 as Visiting Chevron Professor of Energy, March 1 to August 31, 1982 (host W. B. Bridges).

TABLE OF CONTENTS

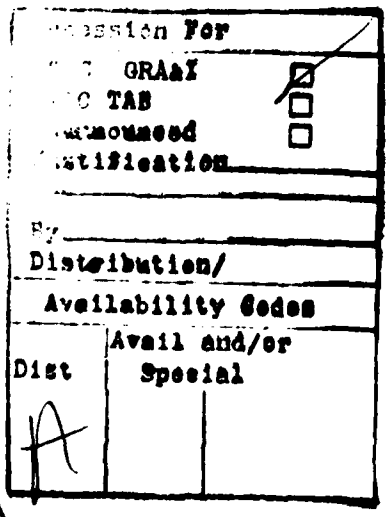

• Indicates ONR supported areas

SECTION I: PLASMA THEORY AND SIMULATION

A. Ion-Ion Two-Stream Mode in a Thermal-Barrier Cell

V. A. Thomas (Dr. W. M. Nevins, LLNL)

We have now achieved a self-consistent equilibrium for our simulation model. In addition to describing the equilibrium model, we wish to indicate some of the important elements of the simulations that will follow later.

Our equilibrium model corresponds to the first physical system that we will study, namely that of a thermal-barrier cell with isothermal Boltzmann electrons (and $T_i \simeq T_e$). These parameters are relevant to the start-up regime for the tandem mirror machine since the heating of the electrons in the plug regions may not have been carried out yet (see the previous QPR for a schematic of the tandem mirror machine and the position of the thermal-barrier cell). Cohen [1] using the results of a Fokker-Planck code created a model distribution function $f(\mu,\epsilon)$ (μ is the magnetic moment and ϵ is the particle energy) for the ions in the thermal-barrier cell that corresponds to this start-up regime. We have generalized this equilibrium by adding a fixed density of hot ECRH electrons that are trapped in the magnetic well of the thermal-barrier cell (these electrons may have to be present before heating in the plug regions has started) . We determine a self-consistent $\phi(x)$ by using a given $B(x)$ and then solving quasi-neutrality:

$$n_i(B,\phi) = n_e(B)_{fixed} + n_{Boltzmann} \exp\left(q_e \frac{\phi}{T_e}\right) \quad .$$

Using this $\phi(x)$ we then use $f(\mu,\epsilon)$ to determine the ion positions, parallel (to the magnetic field) velocities , and μ values (which we take as fixed and use a $\mu \nabla B$ force to simulate the effects of the axial magnetic field) .

To determine if we have a self-consistent solution we then treat the ions as test particles and advance them in the equilibrium fields. If the ion distribution function remains the same as a function of position and the density remains the same our equilibrium solution is correct. We obtain good agreement as shown in Fig. 1 and Fig. 2. An essential feature of this model was pointed out to us by Byers[2] who indicated that each simulation macro-particle should be given a charge weighting proportional to $B(x)$ and therefore the macro-particles should be weighted less in the center of the thermal- barrier cell where B has a minimum. Physically this weighting is a result of the flux tube expansion as the magnetic field becomes weaker. In this sense, even though our model is " 1-d " the other dimensions have not been completely ignored.

In running self-consistent simulations there are several criterion we would like to satisfy. It would be desirable to have $\lambda_{unstable} \ll L$ (here L is the system length) since the unstable wavelengths are on the order of Debye lengths. This means we are going to have to have a great number of particles. We would also like realistic boundary conditions for both the field solve and the particle motion. It may be unnecessary to simulate the entire length of the thermal-barrier since the mode is unstable (locally) only near the center of the cell. This suggests a model where only part of the cell is simulated and the boundary conditions are determined somewhere in the interior of the cell. The amount of the thermal-barrier cell that needs to be retained is still under review. The particle boundary conditions have several possibilities (periodic, specular reflection, random re-injection, etc.). One likely choice is to specularly reflect trapped ions and to use random re-injection for the passing ions. The rationale behind this is that the trapped ions must return to the simulation region after some time that is not too long, whereas the passing ions must travel beyond the thermal barrier cell before they will turn around. These different models for particle boundary conditions need to be examined further before any definite choice is made.

The field solve for these simulations is an iterative solution of Poisson's equation using a fixed density of hot ECRH electrons and a cool Boltzmann component. This field solve was

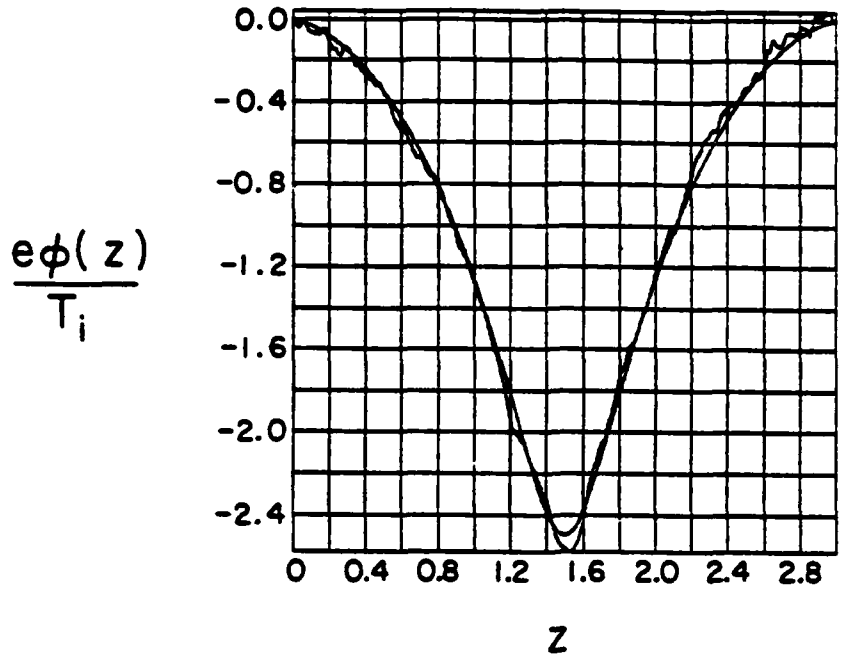

FIG. 1. Equilibrium potential (smooth curve) and the potential from the field solve (rough curve). There are 2048 simulation cells and 100,000 particles. The magnetic field profile is given by the quantity $B(z) = B_{max} - A \sin(2\pi z/L)$. B_{max} is the axial magnetic field at the ends of the thermal-barrier cell; A is a parameter determining the minimum value for the axial magnetic field. The hot ECRH electron population is given a bell shaped density concentrated near the center of the thermal-barrier cell.

discussed in the previous QPR in comparison to a quasi-neutral field solve.

In the future we plan to develop a model for nonuniform electron temperature in order to approximate the response situation after start-up (after the ECRH has already been applied to the plug regions). Whether the cool electrons will again be treated as a Boltzmann fluid is still under consideration. We would also like to generalize this work by examing some aspects of two-stream unstable modes with a 2-d model, including finite beta effects if possible.

1. Cohen, R. H., Axial potential profiles for thermal barrier cells, *Nuclear Fusion* 21, 209 (1981).

2. Byers, J. A., private communication

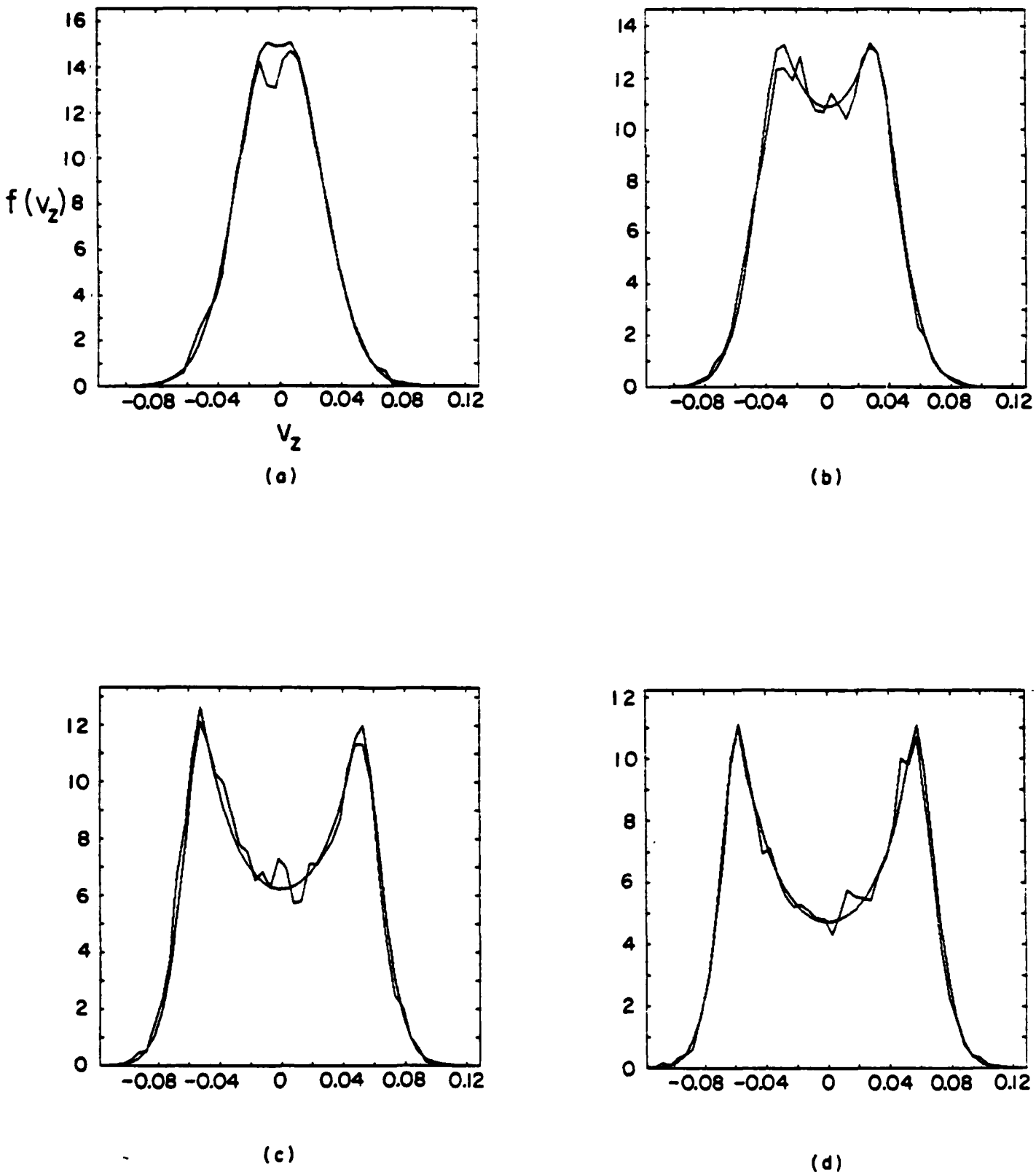

FIG. 2. Ion $f(v_z)$ for : (a) $z = 0$, (b) $z = L/5$, (c) $z = 2L/5$ and (d) $z = L/2$. The smooth curve is the shape from the equilibrium solution and the rough curve is that obtained from the simulation test particles. An average over z was made of 100 grid cells about the given position.

B. Alfvén Ion Cyclotron Instability Particle Simulations

N. Otani (Dr. G. R. Smith, LLNL)

No special progress to report this quarter. See below, in Section II on "CODE DEVELOPMENT" for other work by N. Otani.

C. Time Dependent Child-Langmuir Diode Simulation

S. Rousset (Dr. T. L. Crystal)

An ERL report by this title is in preparation, completing this project, with abstract as follows:

A 1-d numerical code has been written, which allows the time-dependent simulation of the Child-Langmuir diode and the plasma sheath problem. Our model assumes a semi-infinite plasma reservoir from which particles can be emitted into a vacuum region where they can be accelerated or decelerated by means of an external potential on the anode, until they are eventually absorbed by the anode or sent back to the reservoir. Physical results are shown for both the time-independent and the time-dependent cases. Numerical methods are presented for the evaluation of relevant physical quantities. The numerical effects are discussed.

D. Plasma diode: 1-d Vlasov Simulation (GASBAG Code)

Wm. S. Lawson

Purpose

GASBAG is designed to solve electrostatic problems in one dimension with non-periodic boundary conditions. It uses a grid method rather than a particle method, despite the greater simplicity of the particle method, in order to provide an independent check of results obtained by particle methods which are suspected of being numerical or noise effects.

Method

A non-periodic Vlasov simulation poses a major problem for grid solution, because there can be jump discontinuities in the distribution function, which no finite difference equation can adequately handle. To solve this problem, a (hopefully) continuous distribution function is introduced, and a string of test particles is used to keep track of where the discontinuity lies. This is a generalization of the Waterbag model used by Berk and Roberts[1]. This string of particles can be thought of as a line dividing a real distribution function from a fictitious distribution function.

These particles are moved using the standard leap-frog method, which is second order in time. A scheme for moving the distribution function which is compatible with this method of moving the test particles is the splitting scheme used by Cheng and Knorr[2]. This splitting scheme has the advantage that it can be used with any one dimensional method of interpolation (or finite difference approximations to the derivative).

Current Status

All subroutines have been debugged, but most need refinement. The program has been run and debugged, and recent work has centered on finding the best interpolation method. The principle source of inaccuracy stems from the mismatch between the errors in the distribution function, and the errors in the line separating the real part of the distribution function from the unreal part. All the advancing methods for the distribution function have suffered from some degree of either instability, or unacceptable diffusion, resulting in non-conservation of current. I consider errors on the order of 10% to be unacceptable (for most applications), and 1-2% to be acceptable. The following methods have been tried:

Centered derivatives in x and v

This method worked until information had crossed the grid, then went unstable in an odd-even mode.

Uphill-Downhill in x and v

This method works for runs of any length of time, but has diffusion which limits its accuracy to about 10%.

Three point quadratic interpolation in x and v

This method worked to a point, but lead to an odd-even instability around any filamentation, especially around points of a potential minimum.

Three point off-center derivatives in x and v

This method was wildly unstable (as a Fourier analysis shows it should be). A fourth point could be introduced into the finite difference formula to make it Fourier stable. Reducing the time increment might also help.

Three point off-center quadratic interpolation

This method works well, and seems to be the best compromise between accuracy and speed. For single species runs, the accuracy of the final equilibrium was about 1%.

Cubic spline interpolation

This method, like the quadratic interpolation, worked well for a while, then gave rise to

an odd-even mode near the potential minimum.

Present and Future Work

Present work is still focused on finding acceptable methods of advancing the distribution function. A satisfactory method must have very low diffusion over most of the distribution function, but it must diffuse the filamentation (large gradients) or instability will set in.

Further effort will also be spent on improving the diagnostics, and streamlining the code — particularly with regard to the vectorizing abilities of the CRAY-1.

References

1. H. L. Berk and K. V. Roberts, "Nonlinear Study of Vlasov's Equation for a Special Class of Distribution Functions", *Phys. Fluids* **10**(1967), 1595.

   K. V. Roberts and H. L. Berk, "Nonlinear Evolution of a Two-Stream Instability", *Phys. Rev. Letters* **19**(1967), 297.

2. C. Z. Cheng and Georg Knorr, "The Integration of the Vlasov Equation in Configuration Space", *J. Comp. Phys.* **22**(1976), 330-351.

E. Weak Monotonic Double Layers

Mr. Kwang-You! Kim (Dr. T. L. Crystal)

An ERL report by this title for this new project is in preparation, with abstract as follows:

Analytic solutions for two types of double layers are presented: one related to the electron solitary hole (electron phase space vortex), the other related to the ion acoustic solitary hole (ion phase space vortex). We present a derivation of the evolution equation which describes the asymptotic behavior of the ion acoustic double layer having supersonic or subsonic velocity depending on the drift velocity of the cold ions.

Section I. Contribution F.

1982 IEEE INTERNATIONAL CONFERENCE ON PLASMA SCIENCE

MAY 17-19, 1982

Plasma Sheath Formation, Ion Acceleration, and Fluctuations in "Steady" State. C. K. Birdsall, Institute of Plasma Physics, Nagoya University, Nagoya, Japan (EECS Dept. U.C. Berkeley, Calif., U.S.A.)

Sheath formation and subsequent "steady" state near a floating probe (absorbing wall) are observed using simulation with particle ions and particle electrons. An object is to check existing probe theories which have various approximations and to find whether the average of the time-dependent results are close to those of time-independent theory.

The model uses a warm plasma with $T_e \gg T_i$, with m_i/m_e = 1, 25, 100, 400, and 1600. Initially the warm plasma is uniform and quiet (no noise). At t = 0 the absorption begins. The sheath formation is observed first and then the fluctuations in "steady" state are seen. The ions are accelerated toward the probe over a region many λ_{D_e} long and are collected at a velocity $\alpha\sqrt{KT_e/m_i}$, $1 < \alpha < 2$, as expected from fluid theory. However, the floating (or unconnected) probe potential is observed to oscillate at high frequency (very close to ω_{pe}) with large amplitude, on the order of several KT_e/q. The net charge absorbed also oscillates, but at lower frequency and with relatively smaller sawtooth waveform, with short-time electron collection and longer-time ion collection.

Hence, electron dynamics ($m_e \neq 0$) play a large role in determining the fluctuations and time-average behavior of the sheath in these models, which are electrostatic and one-dimensional, so far with lengths up to 200 λ_{D_e} between the particle absorbing and particle reflecting wall(s).

The code ES1 of Langdon[1] with a fast Fourier transform Poisson solver is employed, modified to use superposition for the E field due to the charge on the probe, in order that the computational grid may handle the field due to the plasma charge density more efficiently, typically with wavenumbers k in the range $0.03 < k\lambda_{D_e} < 1.2$ or larger. The initial particle distributions are well ordered in x, v (quiet).

The diagnostics used include the usual quantities (density, potential, field, phase space) plus the ion and electron distribution functions in the plasma and several velocity moments and fluxes of the collected particles.

1. C. K. Birdsall and A. B. Langdon, Plasma Physics via Computer Simulation, McGraw-Hill, N. Y., 1983.

Section I. Contribution G.
Poster Paper presented at International Conference on Plasma Physics 1982
Göteborg, Sweden. June 9-16, 1982

Sheath Formation and Fluctuations with Dynamic Electrons and Ions

Charles K. Birdsall, Inst. of Plasma Physics, Nagoya Univ., Nagoya 464, Japan;
on leave from EECS Dept., Univ. of Calif., Berkeley CA, USA

Abstract: The dynamic behavior of a warm plasma near an absorbing wall, or floating probe, is simulated using particle ions and electrons with mass ratios ranging from 1 to 1600 and temperature ratios, from 1/2500 to 64. The results differ from some time-independent analyses.

1. Physical Model The 1d model is shown in Fig. 1 in x-v_x phase space. The center plane is a floating probe which absorbs ions and electrons from the plasma (A) and the edge planes are elastically reflecting walls (R). Initially, the region $0 < x < L$ is uniformly filled with warm ions and electrons. At $t = 0$, the probe begins collecting charges. The net system charge is always zero so that the net electric flux is zero; there is no applied field. Hence $E = 0$ at $x = 0, L$; by symmetry $E = 0$ at $L/2$. For convenience, potential $\phi = 0$ at $x = 0, L$.

Figure 1.

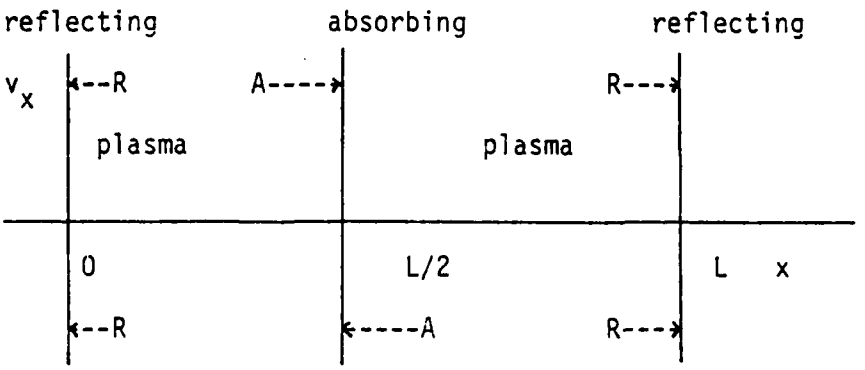

2. Typical Behavior; Prototype Parameters, $T_i/T_e = 1/2500$

$\omega_{pe} = 1$, $v_{te} = 1$, $q_e = -1$, $m_e = 1$; $\lambda_{De} = 1$, $KT_e = m_e v_{te}^2 = 1$.

$\omega_{pi} = 0.05$, $v_{ti} = 0.001$, $q_i = 1$, $m_i = 400$; $v_s = \sqrt{KT_e/m_i} = 0.05$.

The spatial behavior of ρ, E, ϕ, and v_x at $t = 200$ is shown in Fig. 2. The temporal behavior of the probe potential and charge is shown in Fig. 3. The

Figure 2

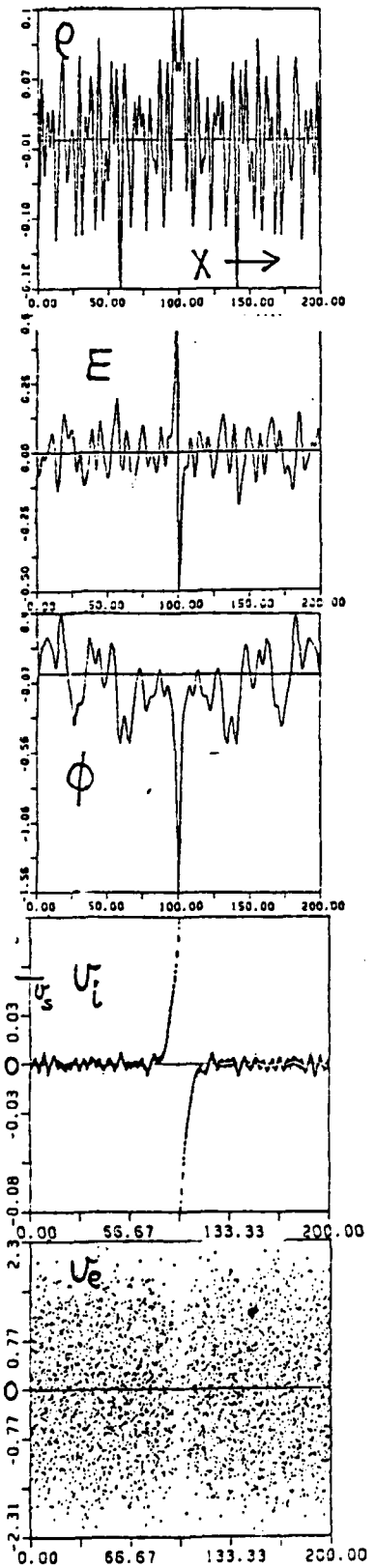

Figure 3

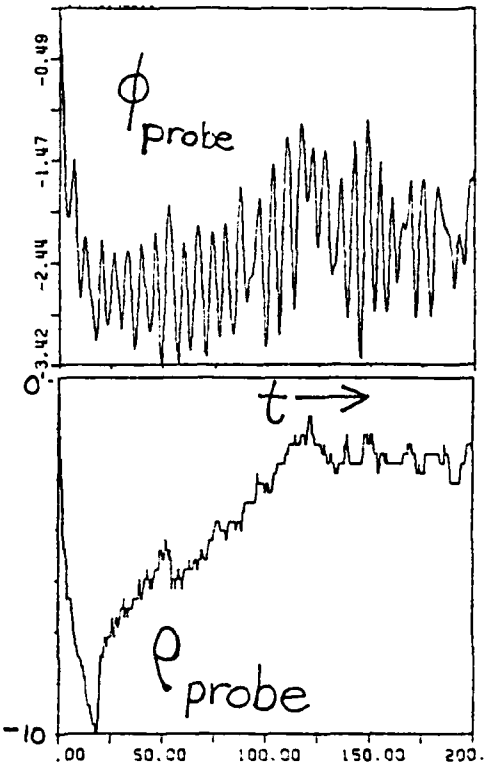

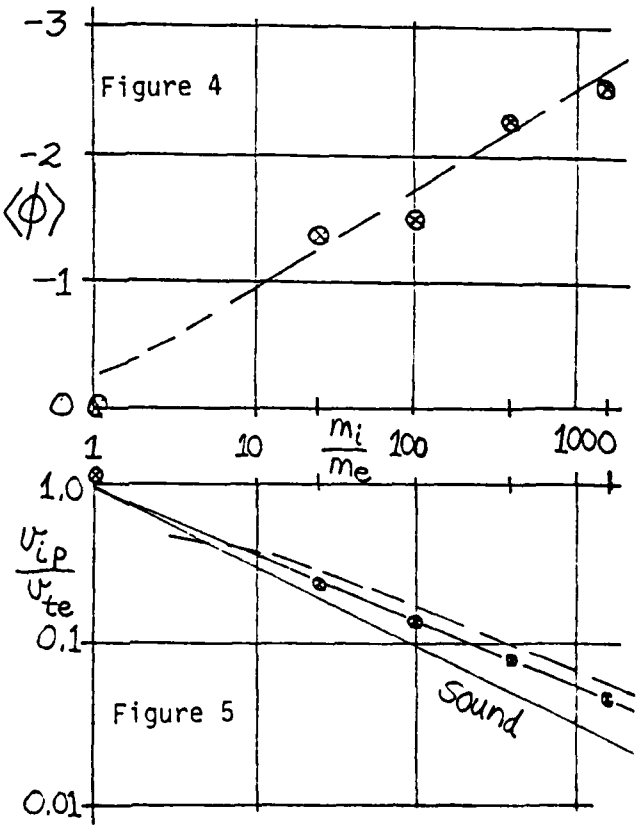

ions begin acceleration toward the probe many λ_{D_e} away where the flow velocity is much less than v_s and are collected at the probe at a velocity v_{ip} nearly twice v_s, in some contrast with time-independent modelings. After the probe charge and potential go negative early, the potential (in units of $e\phi/KT$) oscillates with large amplitude at ω_p about a mean value $<\phi>$. The dependence of $<\phi>$ on m_i/m_e is shown in Fig. 4. The dashed line shown is $e\phi/KT$ from analysis assuming equal fluxes at the probe (from e and i) with zero initial velocity for the ions.

3. Ion Speed at Probe; Dependence on m_i/m_e, for $T_i/T_e = 1/2500$

The ion speed at collection at the probe v_{ip}, for the period t = 160 to 200, is plotted as a function of m_i/m_e in Fig. 5. The distribution about v_{ip} is narrow. v_{ip} is seen to be much larger than v_s with a mass dependence more like $(m_i/m_e)^{0.4}$ than square root. Equal flux analysis produces larger values of v_{ip} than seen but with about the same mass dependence (dashed line).

4. Ion Speed at Probe; Dependence on T_i/T_e for $m_i/m_e = 400$

As T_i is increased, v_{ip} increases as measured in the interval t = 160 to 200, shown in Fig. 6. The mean speed increases toward v_{ti} and the distribution broadens widely. $<\phi>$ goes from -2.25 (prototype) to -0.85 at $T_i/T_e = 16$.

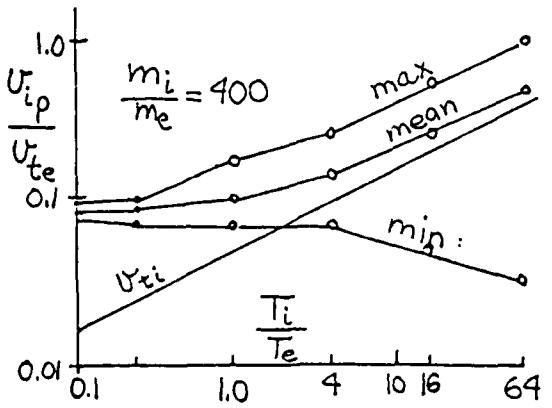

Figure 6

5. Large Amplitude Waves; Model with Disk Charges, Finite Radius

The large oscillations of ϕ suggests that the probe is launching large amplitude waves continually. To check this presumption and the effect of finite radius charges, disks, the code was modified by making $\omega_p^2 \rightarrow \omega_p^2 k^2/(k^2 + (2.405/R)^2)$ where R is the radius of disk charges within a conducting cylinder. For L/R from 0 to 100 with $R > \lambda_{De}$, the sheath behavior is little changed; for larger L/R the cylinder shielding dominates. With a single species, when a strong localized E is applied for about $\tau_p/2$, large amplitude waves leave the source region with little distortion with $v_{phase} = v_{group} = \omega_p R/2.405 + \delta$. With two species it is speculated that these large amplitude waves and large amplitude ion sound waves are launched. The correspondence between the pulsed and continuous model continues.

6. Computer Model Parameters; Variations

The prototype model has NG = 512 cells and N = 4096 particles for each species. The code is ES1 of A.B. Langdon with a quiet start particle loader. Many parameters were varied with no serious problems.

7. Acknowledgments

This research is part of a joint IPP-UCB project on plasma-wall interactions by Dr. T. Kamimura and myself. I am grateful for his providing facilities at IPP and for the excellent programming help of Y. Ohara who has been essential to our rapid progress. I am grateful for partial support from IPP through the Japanese Ministry of Education and for sabbatical leave support from the University of California at Berkeley.

8. Caption for added figure, next page

Early evolution of the sheath, with a floating wall at the right and a reflecting plane at the left. The slanted line drawn in advances to the left at v_{sound}. (a) is $\phi(x)$, with Debye shielding behavior near the wall, but with large-amplitude waves launched away from the wall. (b) is the electron f(v) showing early loss of high velocity electrons. (c) is v_x vs. x for electrons, showing drop-off in $n_e(x)$ and $T_e(x)$ in the sheath. (d) is ion f(v). (e) is v_x vs. x for ions, showing ion acceleration to just above v_s at the wall and expansion of the acceleration region toward the left at v_s. This was not a long enough run to observe evolution of a pre-sheath, which needs at least one ion sound transit.

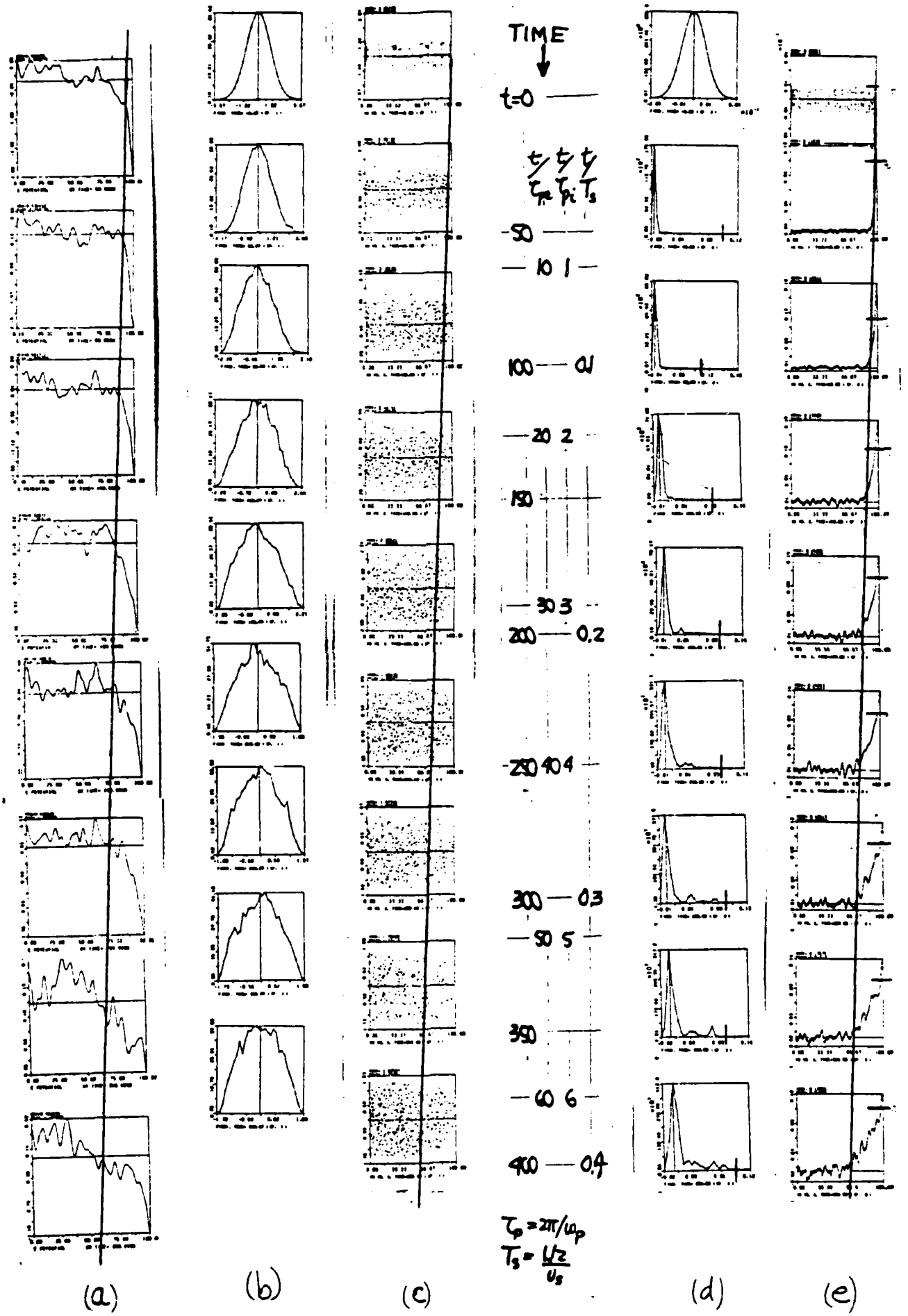
TIME
t=0
t/τ_pe t/τ_pi t/T_s
-50
10 1
100 0.1
20 2
150
30 3
200 0.2
250 4
300 0.3
50 5
350
60 6
400 0.4
τ_p = 2π/ω_p
T_s = L/2 / u_s
(a)
(b)
(c)
(d)
(e)

Paper presented at the Symposium on Plasma Double Layers, Risø Natl. Lab., DK-4000 Roskilde, Denmark, June 16-18, 1982; also, contributions to panel discussic

ELECTRON DIODE DYNAMICS; LIMITING CURRENTS; PLASMA DIODES

Charles K. Birdsall
EECS Dept., Cory Hall, University of California
Berkeley, CA 94720 U.S.A.

Abstract

This paper is intended to complement the papers on double layers, in bringing out the work in the past on virtual cathodes and on limiting currents. The view is that a double layer might be considered to be a virtual cathode for electrons adjacent to a virtual anode for ions, coupled by the shared fields and passing particles. In this view, the formation of a double layer is taken to be the onset of current limiting.

Introduction

It is possible to view double layers as some form of back-to-back virtual cathode and virtual anode, with electrons largely reflected by the former and ions by the latter. The passing particles form the current and are controlled by the fields in the double layer. It may be possible to learn something about double layers by reviewing some of what is known about virtual cathodes. This is one purpose of this paper.

The studies of virtual cathodes show that they are almost always in motion, with the potential minimum oscillating at something like the plasma frequency, both in position and in potential. For cold beams of electrons, this behavior is so pronounced as to make the time average of the time-dependent results (in simulations) quite different from those predicted by time-independent analysis. Hence, we will concentrate in the time-dependent analyses and simulations. For warm beams, the differences are smaller.

Model

The model most commonly used is one-dimensional (1d), bounded at the two ends, x = 0, x = L, by planar grids, which may or may not be connected to external circuits, as shown in Figure 1

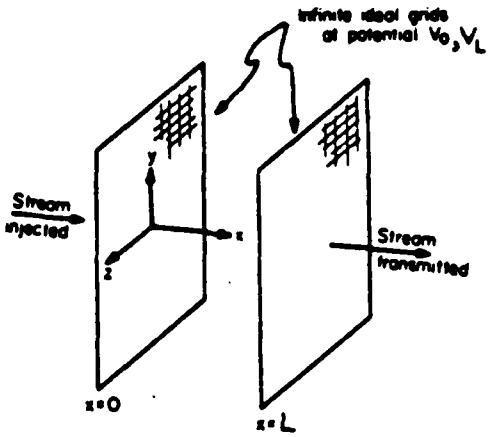

Figure 1. Planar diode model.

Let us use this model to demonstrate a number of results.

Child's Law Diode

The planar electron diode, with a cathode emitting electrons from rest at the cathode at x=0 where $\phi=0$ produces a current density at the anode at $\phi=V_L$ as found by Child (1911), given by

$$J = -(4/9)e_o(-2q/m)^{1/2}V_L^{3/2}/L^2 \quad , \text{ or } \quad w_{pL}L/v_L = (2/9)^{1/2} = 0.4714$$

or a current for a beam radius of R, given by

$$I/V_L^{3/2} = -2.33\times10^{-6}\pi R^2/L^2$$

where this quantity is called the perveance, a geometric factor. Physically, the cathode is a copious emitter, injecting $-J_e$ which greatly exceeds the current transmitted, unless V_L is raised so high as to collect all charge emitted. Langmuir (1923) solved the same model but with a cathode emitting electrons with a half-Maxwellian velocity distribution, with temperature that of the cathode, T; the new feature was the separation of the diode into the α region with charge flowing out and back to the cathode and the β

region, with charge flowing just to the anode, with a potential minimum at the common boundary, as shown in Figure 2. x_{min} is about a Debye length.

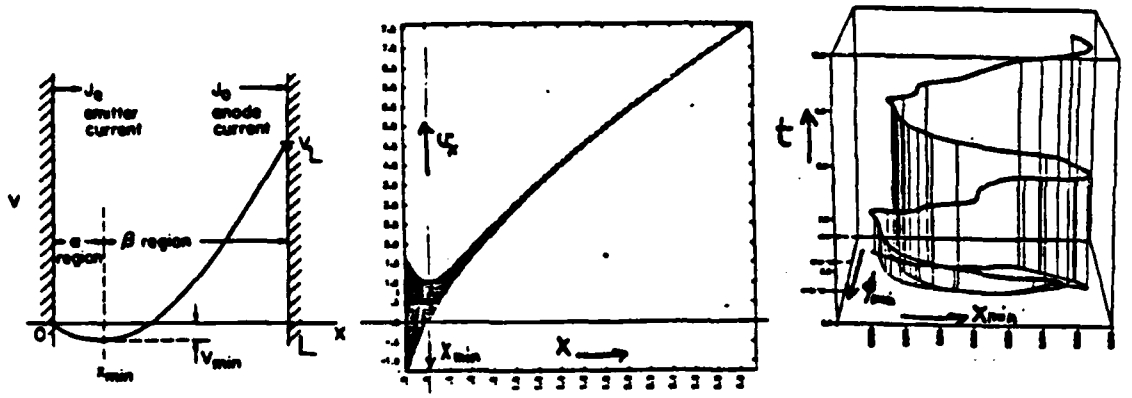

Figure 2 (a) Langmuir warm emitter, with two-directional flow in α, one in β; (b) v_x-x phase space, with both flows, for $eV_L/KT \gg 1$; (c) time history of the minimum potential and position with period about $w_{p,min}$

For the case where the diode is shorted, with both electrodes at $\phi=0$, the phase-space appears as in Figure 3. Note that there are "critical" particles which just reach x_{min} and must decide to go on or turn back, known for a long time to be crucial in noise properties of beams (see Birdsall and Bridges 1966, Ch.6).

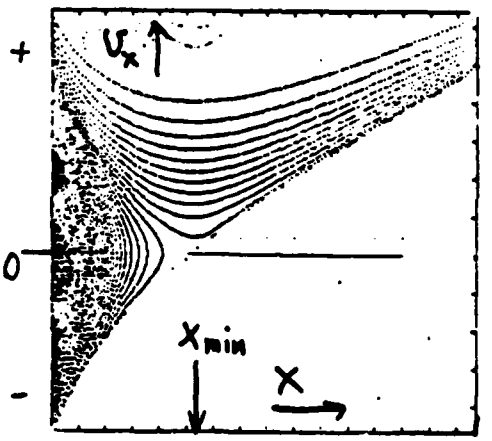

Figure 3

Llewellyn (1941) systematized perturbation analyses for electron diode regions, producing equivalent circuits with admittance $1/z = y = g+jb$, such as shown in Figure 4(a), with results for the Child's Law diode in(b).

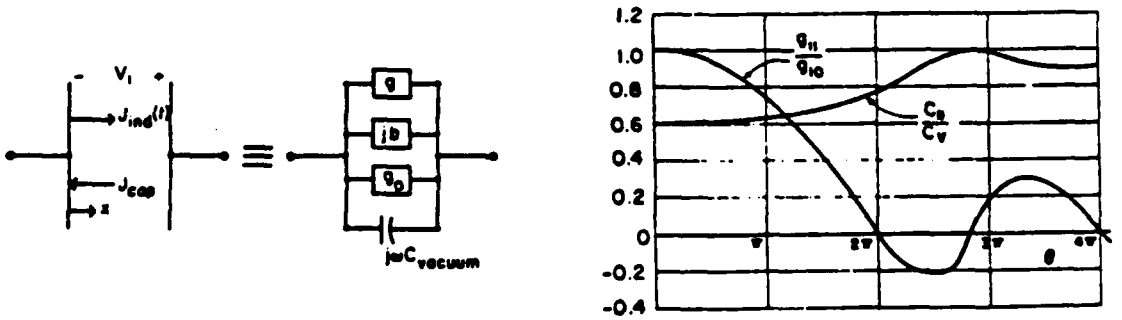

Figure 4 (a) possible equivalent circuit for diode; (b) elements of such a circuit vs. transit angle $\theta = wT$, where $T = L/3v_L$, the transit time.

Note that the conductance can be negative for transit angles $2\pi < \omega T \lesssim 3\pi$; that is, the diode is unstable and will produce oscillations starting from noise. His methods and extensions are given in Birdsall and Bridges(1966).

Fay, Samuel, and Shockley (1938) and Salzberg and Haeff (1938) solved the electron diode behavior for injection of a cold beam at velocity v_o. For example, with $V_0=V_L$, they found that the transmitted current J_T equalled that injected, J_I, up to $J_I = 8J_{Child}$, with unidirectional flow; for larger injection, they postulated two-directional flow and found new virtual cathode solutions with less than half as large J_T, as shown in Figure 5, with an arrow indicating the possible connection between the two solutions (making a hysteris loop), sometimes called the "6L6 effect" after a misbehaving power tetrode. At the maximum current $\omega_{PL}L/v_L = (16/9)^{1/2} = 1.33$.

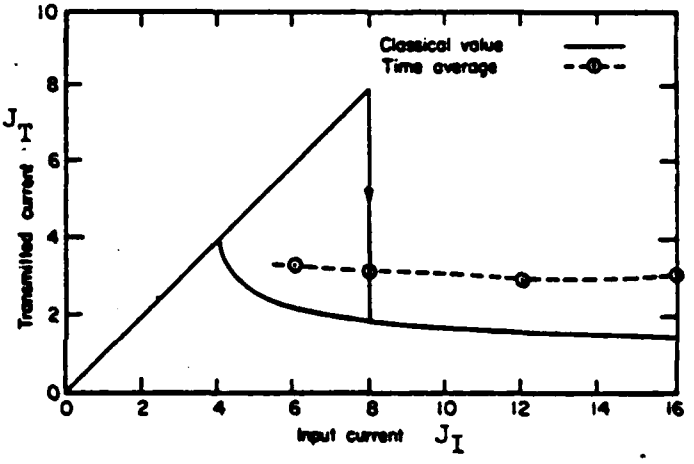

Figure 5

Birdsall and Bridges (1961,1963,1966 in Chap.6) found instability at $8J_{Child}$ from Llewellyn's equations and using particle simulations, showed that after initial pure exponential growth in time, there is an oscillating $\phi_{minimum}$ and oscillating J_T with time average <u>twice</u> that from the above analyses, as shown dashed in Figure 5. For warm beam injection, the oscillation amplitude is smaller and the instability less violent, like Figs.2,3.

Pierce (1944) analysed injection of a cold beam into a short-circuited dioe with a background of immobile ions for neutralization, finding instability at $\omega_p L/v_o = \pi$, about 5.6 times the current for instability of the unneutralized electron diode; adding finite ion mass, Pierce (1948) found

electron-beam-caused growth in space (complex k) a little below w_{pi} and Buneman (1958) solved the same dispersion relation for complex w (hence the name Buneman instability). Pierce (1950) applied his 1948 results to his 1944 diode work, finding the same point of marginal stability. Frey and Birdsall (1965, 1966) also used mobile ions for the neutralized diode (and drift tube) and found the surprising result of no instability, a mistake that was corrected by Faulkner and Ware (1969) who found both the diode and beam-ion instabilities (their ion waves), also making ties to arc-starvation.

Birdsall and Bridges (1961) postulated that the low frequency oscillations (at about ion transit periods) observed in plasma diodes (Cs filled thermionic converters) were triggered by limiting electron currents, with high frequency oscillations (near w_p) which lowered the average potential making a well as seen by the ions; these would then quench as the ions sloshed and filled the well (with w_{pi} or ion transit time oscillations). Cutler (1964) observed a sequence of electron-then-ion plasma oscillations experimentally in a plasma diode. Burger (1964,1965) and Cutler and Burger (1966) provided considerable exmerimental and simulation results on the sequence and on two-time scale oscillations observed in plasma diodes near electron saturation current.

In studying sheath formation near a floating wall, Birdsall (1982) observes much of the above physics in simulations, such as initial wall charging (electron) current, followed by nearly equal electron and ion fluxes, a drop in $\phi(x)$ (at $w_p t = 20$, the maximum drop has occurred, $e\phi/KT_e$ of about -2 or -3 for m_i/m_e of 100 to 400) rising later, a drop in $n_e(x)$ and $n_i(x)$ near the wall, ion acceleration to about v_s or $2v_s$ (over the whole range of T_i/T_e, small to large); the somewhat new results are large oscillations of ϕ_{wall} at w_p, with the ion acceleration region moving away from the wall at speed v_s, with the plasma eventually disappearing (no source is

present, yet). An object is to see whether electrons are collected in bunches, over short intervals, with ion collection over longer periods, producing both high and low frequency oscillations, still with zero net time average flux. Another object is to resolve the differences between time independent analyses and these time-dependent results.

Acknowledgments

I am grateful to the conference leaders for admitting my late paper, to my hosts this sabbatical year, Dr. T. Kamimura at I.P.P. Nagoya, Japan, and Profs. R.W. Gould and W.B. Bridges at Calif. Inst. Tech, Pasadena, CA. Figures 1,2a,4a,b,5 are from Birdsall and Bridges(1966);2b,c from Rousset, U.C. Berkeley, unpublished, with thanks.

References

1911 Child, C.D., Discharge from hot CaO, Phys. Rev. Ser.I 32 492-511
1923 Langmuir, I., The effect of space charge and initial velocities on the potential distribution and thermionic current between parallel plane electrodes, Phys. Rev. 21, 419-435.
1938 Fay, C.E., A.L. Samuel and W. Shockley, On the theory of space charge between parallel plane electrodes, Bell Syst. Tech., 17, 49-79, January
Salzberg, B. and A.V. Haeff, Effects of space charge in the grid-anode region of vacuum tubes, RCA Rev.3,336,Jan.
1941 Llewellyn, F.B., Electron Inertia Effects, Cambridge Univ. Press, London and New York.
1944 Pierce, J.R., Limiting stable current in electron beams in the presence of ions, J. Appl.Phys. 15, 721-726,Oct.
1948 Pierce, J.R., Possible fluctuations in electron streams due to ions, J. Appl. Phys. 19, 231-236, March.
1950 Pierce, J.R., Note on stability of electron flow in the presence of positive ions,J.Appl.Phys., 1[illegible]3,Oct.
1958 Buneman, O., Instability, turbulence, and conductivity in current carrying plasma,Phys.Rev.Let.1,8-9,July 1.
1961 Birdsall , C.K. and W.B.Bridges, Space-charge instabilities in electron diodes and plasma convertors, J. Appl. Phys.,32, 2611-2618 Dec.
1963 Bridges, W.B. and C.K.Birdsall, Space charge instabilities in electron diodes, II, J.Appl. Phys.34, 2946, oct.
1964 Cutler, W.H., High-frequency oscillations in a thermal plasma, J.Appl. Phys.,35,464-465.
Burger,P., Nonexistence of dc states in low-pressure thermionic converters, J.Appl.Phys. 35,3048.
1965 Burger, P.,Theory of large-amplitude oscillations in the one-dimensional low-pressure cesium thermionic converter, J. Appl. Phys., 36, 1938-1943, June
Frey, J.and C.K. Birdsall, Electron stream instabilities with elastic collisions,J.Appl.Phys.36,2962, Sept.
1966 Frey, J. and C.K. Birdsall, Instabilities in a neutralized electron stream in a finite-length drift tube, Jour. Appl. Phys., 37, 2051-2061, April
Birdsall, C.K. and W.B. Bridges, Electron Dynamics of Diode Regions, Academic Press, New York.
Cutler, W.H., and P. Burger, Oscillations in the thermal cesium plasma diode, J. Appl.Phys.,37,2867, June.
1969 Faulkner, J.E. and A.A. Ware, The effect of finite ion mass on the stability of a space-charge-neutralized diode, J. Appl. Phys., 40, 366, June.
1982 Birdsall, C.K., Sheath formation and fluctuations with dynamic electrons and ions, Int. Conf. Plasma Physics, Göteborg, Sweden, June.

Remarks by C.K. Birdsall at panel discussion, Risø Symposium on Double Layers

A ten year background (the 1950's) using electron beams for microwave devices provides me with numerous pre-conceived notions towards double layers, sheaths and freely expanding plasmas. Some of these may be wrong, some may not be applicable and a few may be helpful.

Suppose that a double layer with potential increasing to the right is

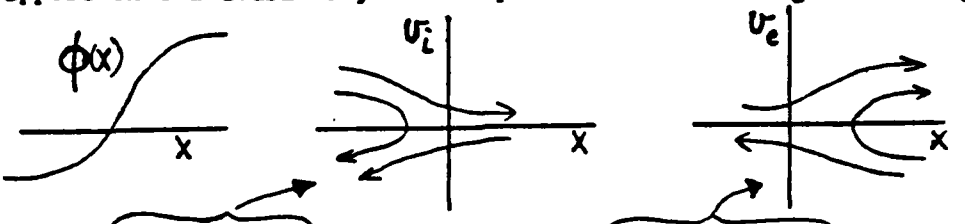

viewed as a virtual anode on the left and a virtual cathode on the right, coupled together by the passing particles and the electric field. In this view we expect to observe oscillations or enhanced noise at about w_{pi} near the virtual anode (where ions are turned around) and similar at about w_{pe} near the virtual cathode (where electrons are turned around). Indeed, Ch. Hollenstein showed experimental results of this kind, here.

Such expectations come from old experience, both experimental and with simulation, with isolated virtual cathodes (or anodes) which were produced by limiting-current instabilities, in electron (or ion) diodes, with or without applied potential differences. These instabilities have thresholds given in terms of normalized lengths, such as $w_p L/v_{Beam}$ = constant, where the constant depends on whether the beam is cold or warm, on whether the beam is neutralized and that on whether the neutralizing is mobile or not.

The thresholds for formation of double layers may have similar form, somewhat as hinted at the meeting in terms of minimum L/λ_D; such thresholds as reported may need refining in terms of v_{Beam} and $v_{thermal}$.

It appears desirable to devise models for the laboratory and for simulation with similar parameters (paired) in order to check these views in some detail. This is an appeal to obtain detailed understanding of even the simplest models. Such knowledge may then be brought to bear on more complex models as exist in space plasmas or in fusion plasma devices, such as tandem mirrors, with multi-kilovolt potential wells.

My thanks to Dr. L. P. Block for providing a dozen or more stimulating statements to the panel and audience, and for the invitation to serve on the panel.

SECTION II: CODE DEVELOPMENT

A. Availability of ZED Postprocessor on MFE-CRAY Computers

Niels F. Otani (Dr. W. M. Nevins, LLNL)

The ZED Postprocessor, previously available on MFE's CDC-7600 computer, has been modified to run on MFE's CRAY computers. The most recent working version of this CRAY/ZED may be obtained from CRAY/FILEM by typing:

filem rds 30143 .crayzed zed

The current version, to which this report applies, was compiled from a source (sourcename = *szed*14*f*) which can also be found in the same FILEM directory.

Operation of ZED on the CRAY is identical to operation on the CDC-7600, with the following exceptions:

1) The "control-E-I" interrupt is not yet operational in the input line, and while not fatal, produces strange behavior if invoked while the code is attempting to send graphics.

2) The user must wait for the *second* bell prompt following graphics output (i.e., after drawing a plot on the screen) before attempting to enter another command line. (The first bell belongs to NETPLOT.)

3) The TV*nnn* command has been replaced with the GUSS-compatible commands "tvon*nnnnn*" and "tvoff".

4) Labels, numbers, etc. (except box and ID) must be eight characters or less in length, since CRAY words are only eight characters long.

5) The format of the *state* file has been changed. It is now solely dedicated to providing parameter information to ZED. The *history* file is similar in structure to its CDC-7600 counterpart, differing only in that it uses CRAY-format for its integer, floating-point and octal labels.

6) The NA option in the "plot" command causes the current frame to be plotted with the preceding frame instead of with the following frame.

7) The default site associated with the "print" command is the same as NETPLOT's default site.

8) Blank common takes the place of large core memory for the commands "makebuf", "save", and "dumpbuf".

9) The integer associated with the "tekon" command is the baud rate as understood by NETPLOT (see the NETPLOT document).

10) Two additional commands have been added: "file" and "pause", which allow the use of command input files.

Summary of ZED Commands

For the reader's convenience, a summary of ZED commands is presented here. While including all ZED commands, this summary is not meant to be complete; the reader is referred to the original ZED documents for more detail and definition of terms.

In the following, square brackets enclose optional input specifications.

To start the ZED program, type:

zed [*history* [*state*]]

where *history* is the name of the history file and *state* is the name of the state file. If *history* is omitted, ZED assumes a history file named "history" and a state file named "state". If *state* is omitted, no state file is assumed, and parameters must be entered manually by the user. In particular, the STEPS command must be used.

(1) ZED Operating Commands

When ZED prompts with ".", any of the following ZED commands may be entered:

end

Terminates the ZED program and closes all files.

x

Null command.

loop *var* = *nl nu step*

where *var* is a user supplied dummy variable name and *nl*, *nu*, and *step* are integers.

Allows the user to execute several commands, incrementing *var* in the command expressions each time.

esc
linefeed

where *esc* is the escape character and *linefeed* is the linefeed character.

Allows the user to stack several commands on a single line using *esc* or *linefeed* as delimiters.

file *filename* [*linenum*]

where *filename* is a command input file, and *linenum* is the line at which ZED will begin reading the file. If *linenum* is not specified, ZED starts at the beginning of the file.

This command causes ZED to fetch subsequent commands from the command input file until one of the following occurs: (1) an illegal command format is encountered, (2) the user interrupts with "control-E-I", or (3) ZED reaches the end of the file. The input file may contain any legal sequence of ZED commands including the "loop" command. The only restrictions are that commands may not be stacked (i.e. use only one command per line), and that use of the "file" command may quickly result in chaos. Plots will bee sent to the Tektronix terminal or GUSS monitor if enabled.

pause

This command is intended for use in a comn and input file, following a "plot" command. It causes a delay, allowing the user to view the current plot with some leisure.

(2) ZED Operating-Parameter Specification Commands

modes

Commands ZED to read the "modes" portion of the history for the remainder of the session.

steps *il iu* [*iskip*]

where *il*, *iu*, and *iskip* are integers.

Indicates to ZED which timesteps reside in the history file.

id

Allows the user to change the box and ID.

var = *val*

where *var* is the name of a variable residing in the namelist ZEDIN and *val* is a floating-point number in F-format or an integer.

Assigns the value *val* to the namelist variable *var*. Currently namelist ZEDIN contains the following variables: ilw, idw, iwf, wmaxs, ny, dt, dgamma, ixl, ixu, ixskip, and dx.

xmodes *tv ix iy*

where *tv ix iy* is a mode record label.

Informs ZED that the current history file contains cross-spectrum/cross-correlation information with record "*tv ix iy*".

movie

Initiates the plot output file for the generation of 16 mm sprocketed movie film and writes a film header. This routine has not been tested in the CRAY version.

(3) Data Specification Commands

? [*ir*1][*ir*2][*ir*3] ...

where *ir*1, *ir*2, *ir*3 ... are internal record numbers.

Asks ZED to print the contents of internal records *ir*1, *ir*2, *ir*3 ...

label *ir ix iy* [&]

where *ir* is an internal record number and *ix* and *iy* are integers.

Commands ZED to label internal record *ir* with mode record label "50 *ix iy*". The following record is also labeled when "&" appears.

(4) Data Transfer Commands

read [*var*1][,][*var*2][,][*var*3][,] ...

where *var*1, *var*2, etc. are record labels in the history portion of the history file.

Before the "modes" command, reads *var*1 into internal record 1, *var*2 into internal record 2, etc. If, say, *var*2 is omitted, *var*3 is still read into internal record 3, while nothing is read into internal record 2, demonstrating the comma's role as placeholder.

read [*tv*1 *ix*1 *iy*1][,][*tv*2 *ix*2 *iy*2][&][&][&] ...

where *tv*1 *ix*1 *iy*1, *tv*2 *ix*2 *iy*2, etc. are mode record labels of records residing in the modes portion of the history file.

After the "modes" command, reads "*tv*1 *ix*1 *iy*1" into internal record 1, "*tv*2 *ix*2 *iy*2" into internal record 2, etc. As above, commas may be used as placeholders. The "&" requests that the following record(s) in the modes portion of the history file be read into

subsequent internal records. If "xmodes *tv*4 *ix*4 *iy*4 " was previously specified, "read *tv*1 *ix*1 *iy*1" reads the cross-spectrum/cross-correlation record *tv*1 *ix*1 *iy*1 *tv*4 *ix*4 *iy*4.

readx [*tv*1 *it*1 *iy*1][,][*tv*2 *it*2 *iy*2][&][&][&] ...

where *tv*1, *iy*1, *tv*2, *iy*2, etc. refer to mode record labels, and *it*1, *it*2, etc. refer to timestep numbers.

Reads all modes with *tv*1 and *iy*1 at timestep *it*1 into internal record 1, etc. as a function of the x-index *ix*. Commas and ampersands are used as with the "read" command. The increment in *ix* is 1 unless preceded with the command "ixskip = *n*" where *n* is an integer. The lower and upper bounds of *ix*, ixl and ixu, may be set in a similar manner.

tekon [*baudrate*]

where *baudrate* is an integer baud rate.

Allows users having Tektronics graphics terminals to view frames plotted by ZED. To see a plot, the plot command must be last command in a command stack, and must not be a loop command.

tekoff

Disables the interactive Tektronix plotting feature.

tvon *nnnnn*

where *nnnnn* is the GUSS monitor number. Allows users having access to GUSS monitors to view frames plotted by ZED. To see a plot, the same conditions must hold as for the "tekon" command.

tvoff

Turns off GUSS monitor plotting and then releases the monitor.

print [*site*]

Sends all plots produced up to this point to *site*, destroys the plot file, and opens a new plot file. If *site* is not specified, the default site is the same as NETPLOT's.

flush

Empties plot buffers to the plot file so the current plot file may be viewed on another channel. This command is not normally necessary on the CRAY, since the buffer is emptied every frame in the current version.

makebuf *isize* [c]

where *isize* is a positive integer.

Creates a buffer in blank common large enough to hold *isize* records. If "c" is present, enough room is created to hold *isize* complex records (i.e., 2**isize* records).

save *ir*1 [*ir*2] [*ir*3] ...

where *ir*1, *ir*2, etc. are internal record numbers.

Copies internal records *ir*1 *ir*2, etc. into the blank common buffer created by a "makebuf" command.

dumpbuf [*familyname*]

where *familyname* is a user-supplied output filename, mandatory on first call to "dumpbuf".

Creates a ZED-compatible history file named *familyname*0 (or subsequent files named *familyname*1, *familyname*2, etc.), dumps the blank common buffer into it, and eliminates the buffer from memory. This call must be preceded by a "save" command.

next *history*

Closes the current history file and opens *history* as the new history file. No operating parameters are changed.

write

Writes the contents of the internal records to a text file ZED0. This command is used primarily for debugging.

(5) Data Diagnostics Commands

sparam *lw* [*dw* [*wmax*]]

where *lw* is the lag window (integer), *dw* is the data window (integer), and *wmax* is the maximum frequency to display (real).

Sets parameters associated with ZED's Fourier transform routines.

spect *ir*1 *ir*2 [*ir*3 *ir*4]
rcorr *ir*1 *ir*2 [*ir*3 *ir*4]
cspect *ir*1 *ir*2 [*ir*3 *ir*4]
ccorr *ir*1 *ir*2 [*ir*3 *ir*4]

where *ir*1, *ir*2, *ir*3, and *ir*4 are internal record numbers.

The commands "spect" and "rcorr" return the power spectra and autocorrelation functions, respectively, of the two real records *ir*1 and *ir*2. The functions are returned to internal records *ir*1 and *ir*2 unless *ir*3 and *ir*4 are specified. The commands "cspect" and "ccorr" are the same except the real and imaginary parts of one complex record are assumed to reside in *ir*1 and *ir*2.

xspect *ir*1 *ir*2 *ir*3 *ir*4 [*ir*5 *ir*6]
xcorr *ir*1 *ir*2 *ir*3 *ir*4 [*ir*5 *ir*6]

where *ir*1, *ir*2, etc. are internal record numbers.

Calculates the cross-spectra and cross-correlation functions of *ir*1 and *ir*2 with *ir*3 and *ir*4 and stores the result in *ir*1 and *ir*2 unless *ir*5 and *ir*6 are specified.

filter *ir w* [*width*]
rfilter *ir w* [*width*]
cfilter *ir w* [*width*]

where *ir* is an internal record number, *w* is the central frequency (real), and *width* is the frequency width (real).

Applies a bandpass filter at frequency *w* with width *width* to the data in internal record *ir* (and *ir* + 1 in the case of "cfilter"). The command "rfilter" assumes *ir* is a real record, "cfilter" assumes records *ir* and *ir* + 1 comprise a complex record, and "filter" tests to see whether "rfilter" or "cfilter" is appropriate.

mem

Calculates the spectral density of complex data assumed stored in internal records 1 and 2, using the Maximum Entropy Method. The two-time correlation function is returned to records 3 and 4, the response function is returned to records 5 and 6, and the spectral density is returned to records 7 and 8.

r*n* = mod r*m* [r*l*]
r*n* = mod2 r*m* [r*l*]

where *l*, *m*, and *n* are internal record numbers.

Returns to internal record *n* the modulus and square modulus, respectively, of the data stored in record *m*. The imaginary part of the data whose real part is stored in *m* is assumed stored in record *m* + 1, unless r*l* is specified.

r*n* = dif r*m* [δ]

where *m* and *n* are internal record numbers, and δ is "dx", "dt", or "dw".

Returns to record *n* the finite difference derivative of record *m* with respect to *delta*. If δ is not specified, it is determined by the internal data type specification.

r*n* = r*m* *op* r*l*[(*it*)]
r*n* = r*m* *op*[-]*const*

where *l*, *m*, and *n* are internal record numbers, *op* is "+", "-", "*", or"/", *it* is a timestep number (integer), and *const* is a real constant expressed in F-format.

Returns to record *n* the sum, difference, product, or quotient of two other records, or a record and a constant. Note the correct format in the case of a negative constant. If *it* is specified the operation is between record *l* at timestep *it* and record *m* at all timesteps.

(6) Data Generation Commands

gen *ir amp freq phase*
cgen *ir amp freq phase*

Generates a sinusoidal signal of amplitude *amp*, frequency *freq*, and phase shift *phase*. The command "gen" stores a real signal in internal record *ir* while "cgen" stores a complex signal in records *ir* and *ir* + 1.

exp *ir* γ

Stores a real exponential function with growth rate γ (real or integer) in record *ir*.

(7) Plotting Commands

plot *ir* [log][lin][*var*1=*const*1][*var*2=*const*2][cl=*x*][l][na][d]
splot *ir* [log][lin][*var*1=*const*1][*var*2=*const*2][cl=*x*][l][na][d]
xplot *ir* [log][lin][*var*1=*const*1][*var*2=*const*2][cl=*x*][l][na][d]
plotx *ir* [*var*1=*const*1][*var*2=*const*2][cl=*x*][l][na]
ints *ir* [*wmin*][*wmax*]
plotm *ir*

-or-

plot *ir* p
splot *ir* p
xplot *ir* p
plotx *ir* p

where *ir* is the number of the internal record to be plotted, *var*1, *var*2, etc. are namelist variables, *const*1, *const*2, etc. are real constants expressed in F-format, *x* is a single alphanumeric character, and *wmin* and *wmax* are real constants.

If the "p" option is used, ZED will prompt you for plot options.

Explanation of plotting options:

lin : Produces a linear-ordinate plot
log : Produces a log-ordinate plot
var=*const*: Sets plot parameter *var* to value *const*
cl=*x* : Labels the trace of the current record data with character *x*.
l : Causes ZED to prompt for a plot label
na : Plots the current frame with the previous one
d : Produces a dashed trace

Explanation of the individual plotting commands:

plot : Plots data using "splot" or "xplot" if necesary. Otherwise a conventional plot is produced using the the parameter namelist PIN.
splot: Plots spectral data using the parameter namelist SPIN.
xplot: Plots cross-spectrum/cross-correlation data using the parameter namelist XPIN.
plotx: Plots data obtained from the "readx" command using parameter namelist PIN.
ints : Plots the integral of spectral data from *wmin* to *wmax*.
plotm: Plots the real and imaginary parts of complex data assumed to reside in records *ir* and *ir* + 1 in one plot. The modulus of the data is plotted in a second plot.

Current plot namelist variables:

PIN : min, max, tmin, tmax, nplt
SPIN: min, max, wmin, wmax, nplt
XPIN: min, max, xmin, xmax, nplt

B. Generation of Data Files Compatible with the MFE-CRAY Version ZED Postprocessor

Niels F. Otani (Dr. W. M. Nevins, LLNL)

Three routines have been created to facilitate the generation of state and history files compatible with the newly available MFE-CRAY-version ZED Postprocessor. The routines are easy to use--in addition to calling the routines themselves, the user need only supply namelists containing all variables which the user may wish to write, a special array named "modetabl", and an input file at runtime.

The routines, SETFILEZ, WRFILEZ, and WRFILPZ are contained in the binary library BUTILS available from FILEM via:

filem rds 1210 .zed butils butils-s

BUTILS-S contains the sources of the three routines should the user require modification.

SETFILEZ is the initialization routine and therefore should be called before entering the main timestep loop. SETFILEZ is called with the following arguments:

call setfilez (iushist,iusstate,infile,modetabl,dt,ny,ntuu)
where

iushist	: unit specifier to be associated with the history file
iusstate	: unit specifier to be associated with the state file
infile	: name of the input file to be read by SETFILEZ
modetabl	: is an array at least 37b in length (note: 37b means 37-octal), and on input should contain the mode variable names. For example, if the ZED quantity tv = 22b is to be associated with the variable " phi", then the user must set modetabl(22b) = "phi" prior to calling SETFILEZ.
dt	: the timestep size
ny	: dimension of the y- (second) index. Note: ny is only used for ZED labeling conventions and only with (t=3)-type variables. See BUTILS-S for details.
ntuu	:= on exit, contains the last timestep required by these ZED file-writing routines

SETFILEZ reads an input file which the user uses to specify which history and mode variables are to be written. The following typical input file serves to illustrate the input file format:

```
2000 steps from step 100
var1, var2,
var3
var4, var5, var6
every 10 steps
q, 0 5 1, 1
phi, 3, 2
ex, 0 3 3, 1 3 1 &
```

The first line designates that 2000 timesteps beginning with timestep 100 will be monitored by these ZED-interface routines. If the first timestep to be read is timestep 0, the "from step 100" clause may be omitted. The next three lines specify that the (unindexed) variables var1, var2, var3, var4, var5, and var6 are to be written to the history portion of the history file. Note that any number of history variables may be written on one line and that commas are ignored. Any number of lines may be used.

The line with "every" as its first word signals the modes specification portion of the file. The clause "every 10 steps" indicates that modes information will be written to the modes portion of the history file every 10 timesteps. The next three lines illustrate the format used for describing which modes are to be written. Only one mode variable may be specified per line. The range of each of two indices is specified by one or three integers. If one number appears only modes with that value for the corresponding index will be written. If three numbers are indicated, modes within the range defined by the first two numbers (lowest index first) will be

written by increments specified by the third number. If an ampersand appears at the end of a mode descriptor line, the corresponding variable will be assumed to be complex, and the imaginary part of the variable will be stored after the real part in the modes portion of the history file. Note that for one-dimensional arrays the second index is always 1.

The names of the history and state files created by SETFILEZ are, by default, "history" and "state". These names may be changed by accessing the common block CZFNAMES in the user program:

```
common /czfnames/ statenam, histname
```

SETFILEZ allows new ZED files to be created in the same run by 1) closing the old history and state files, 2) assigning new history and state filenames via CZFNAMES if desired, and 3) recalling SETFILEZ. This feature is useful in codes with restart capabilities.

The routines WRFILEZ and WRFILPZ are called in the timestep loop by the user program and perform buffered writes to the ZED files according to specifications passed from SETFILEZ. WRFILPZ writes pointer-designated mode array data, while WRFILEZ writes conventional mode array data. Both routines also write conventional history (unindexed) data. WRFILPZ is specially designed for use with the author's pointer-defined arrays; most users, using conventionally-defined arrays, will want to use WRFILEZ.

Actual disk-writes to the history file are accompanied by corresponding updates of the state file, thus allowing the user to use the ZED postprocessor on the ZED files to monitor progress while the main code is still running.

WRFILEZ and WRFILPZ are called as follows:

```
call wrfilez (it,histnlst,modenlst,itype)
call wrfilpz (it,histnlst,modeptrs,mdim,itype)
```

where

it	: current timestep no.
histnlst	: name of a namelist containing variables to be written into the history portion of the history file at this call
modenlst	: name of a namelist containing arrays to be written into the modes portion of the history file at this call
modeptrs	: name of a namelist containing pointers of the mode array quantities to be written into the modes portion of the history file at this call. Pointer names must be of the form p*var* where *var* is the name of the corresponding mode array.
mdim	: an array of dimension 4. mdim must be filled with the dimensions of all arrays in modeptrs prior to calling WRFILPZ. WRFILPZ will assume all arrays have dimension (mdim(1):mdim(2) , mdim(3):mdim(4)). Important: the values of mdim **must** be correctly set to insure proper writing of the data by WRFILPZ.
itype	: 1 if mode arrays are real : 2 if mode arrays are complex Important: All arrays represented in a mode namelist **must** be of the same type and itype **must** be correctly set to insure the proper array quantities are written. If both real and complex arrays are to be written, the user simply calls WRFILPZ twice, once for each type of array.

Either or both routines may be called more than once in the timestep loop with mutually exclusive namelists, permitting the user to write different mode array types (and different mode array dimensions, in the case of WRFILPZ). This also allows the user to write different variables from different parts of the timestep loop. The same array may even be written more than once in one timestep, by using EQUIVALENCE statements and then including different names for the same array in different namelists. This feature is useful for writing an array and later its Fourier transform stored in the same array.

Simple usage of the ZED-interface routines is illustrated in the following program:

```
      dimension q(0:5), phi(64,64), ex(0:63,0:63), rho(64,64)
      namelist /hnlst/ var1, var2, var3, var4, var5, var6
      namelist /mnlst/ q, phi, ex, rho
      dimension modetabl(37b)
c     Initialize code run:
        dt = 0.2
        (Other initializations required by code)
        modetabl(21b) = "q"
        modetabl(22b) = "phi"
        modetabl(23b) = "ex"
        modetabl(24b) = "rho"
c     Read input file "inzed" and initialize ZED interface routines:
        call setfilez (8,9,"inzed",modetabl,dt,1,ntuu)
c     Main timestep loop:
        do 100 it = 0, ntuu
        .
        .
        call wrfilez (it,hnlst,mnlst,1)
        .
        .
100   continue
        call exit
        end
```

This routine will write history variables var1, var2, var3, etc., and real mode variables q, phi, ex, and rho to a history file named "history" with history file state information written to state file "state" according to specifications contained in input file "inzed".

SECTION III: SUMMARY OF REPORTS, TALKS, VISITS & VISTORS

Reports:

C. K. Birdsall "Plasma-Sheath-Wall Time-Dependent Behavior: An Informal Survey", ERL Memo UCB/ERL M82/51, 22 June 1982.

Talks:

C. K. Birdsall "Electron diode dynamics; limiting currents plasma diodes," Symposium on Plasma Double Layers, Risø National Lab, Roskilde, Denmark, June 16-18, 1982.

C. K. Birdsall "Sheath formation and fluctuations with dynamic electrons and ions," International Conference on Plasma Physics 1982, Göteborg, Sweden June 9-16, 1982.

C. K. Birdsall "Plasma sheath formation, ion acceleration, and fluctuations in 'steady' state," 1982 IEEE International Conference on Plasma Science, Ottawa, Canada, May 17-19 1982 (Paper 1R7 in IEEE Conf. Record).

Visits:

Prof. Birdsall was on sabbatical leave in this period, with visits to and talks at plasma facilities in Osaka, Hiroshima, and Sendai Japan; additional visits to and talks at
(i) Risø National Lab, Denmark (host J-P Lynov),
(ii) Centre de Recherches en Physique des Plasmas, Ecole Polytechnique, Lausanne Switzerland (host C. Hollenstein),
(iii) Culham Lab, England (hosts J. Eastwood and K. Roberts) and
(iv) Reading University England (host R. Hockney).
Trip report for (i-iv) is available.

University of California, Berkeley
Electrical Engineering & Computer Sciences
Plasma Theory and Simulation Group

EECS 298-9: PLASMA THEORY & SIMULATION SEMINARS

Winter 1982	Fridays 3:00-5:00 PM	T.L.Crystal
	Room 297 Cory Hall	642-9672

Jan 22 Garret Jernigan, S.S.L.
New techniques for electrostatic and gravitational simulations.

Jan 29 Vince Thomas
One-dimensional space-charge neutralization of ion beams.

5 Feb Niels Otani
Propagation of waves generated in Tandem Mirror end cells.

12 Feb Jack Byers, LLNL
i. Monte Carlo studies of resonance transport in Tandem Mirrors.
ii. Simple models of magnetic drift pumping.

19 Feb Bill Lawson
Non-particle simulations of Vlasov plasmas.

26 Feb Stephane Rousset
Subroutines for solving stiff sets of ODE : CHEMEQ.

5 Mar Ned Birdsall
Group review and trip report.

12 Mar Kirk Kenyon
Computer modelling of RF heating.

19 Mar Kwang-Youl Kim
Dynamics of solitons in plasmas.

All are invited to join us for wine afterwards (it's Friday after all).

Electrical Engineering & Computer Science Department

EECS 298-9 SEMINAR: PLASMA THEORY & SIMULATION GROUP

Spring 1982 — Fridays 3:00-5:00 PM — Room 395 Cory Hall — T.L.Crystal 642-9672

9 April Kwang-Youl Kim
Soliton fundamentals: part 1

MONDAY 19 April (Combined into Physics 290A sec 2 plasma seminar)
Bruce Cohen, LLNL
Drift cone simulations in a neutral beam driven mirror

23 April Mike Gerver, M.I.T.
Trapped-particle modes in tandem mirrors

30 April Yu-Jiuan Chen, LLNL
High frequency microinstabilities in hot electron plasmas

7 May Vince Thomas
Different models for the electron population in simulations

14 May Mark Kushner, LLNL
A kinetic view of plasma etching

21 May Stéphane Rousset
MHD particle simulations with Lax-Wendroff algorithm

28 May Niels Otani
to be announced

4 June Kirk Kenyon
Rings and spokes: instability simulation problems

11 June Kent Estabrook, LLNL
Finite-difference methods of solving the Vlasov equation

All are invited to join us for wine (or soft-drinks) provided afterwards.....it's Friday after all!

DISTRIBUTION LIST

Department of Energy
Hitchkock, Katz, Lankford, Nelson, Sadowski

Department of Navy
Condell, Florance, Roberson

Austin Research Associates
Drummond, Moore

Bell Telephone Laboratories
Hasegawa

Cal. Inst. of Technology
Liewer

Calif. State Polytech. Univ.
Rathmann

Cambridge Research Labs
Rubin

Columbia University
Chu

E. P. R. I.
Scott

General Atomic Company
Bernard, Helton, Lee

Hascomb Air Force Base
Rubin

Hughes Aircraft Co., Torrance
Adler, Longo

Hughes Research Lab, Malibu
Harvey, Poeschel

JAYCOR
Hobbs, Klein, Tumolillo, Wagner

Kirtland Air Force Base
Pettus

Los Alamos National Lab.
Barnes, Borovsky, Forslund, Kwan, Lindemuth, Mason, Mostrom, Nielson, Oliphant, Sgro, Thode

Lawrence Berkeley Laboratory
Cooper, Kaufman, Kim, Kunkel, Lee, Pyle

Lawrence Livermore National Lab.
Albritton, Anderson, Brengle, Briggs, Bruijnes, Byers, Chambers, Chen, B.Cohen, Denavit, Estabrook, Fawley, Friedman, Freis, Fuss, Harte, Killeen, Kruer, Langdon, Lasinski, Maron, Matsuda, Max, Nevins, Nielsen, Smith, Tull

Mass. Inst. of Technology
Berman, Bers, Gerver, Hewett,

Mission Research Corporation
Godfrey

Naval Research Laboratory
Boris, Craig, Haber, Orens, Winsor

New York University
Grad, Harned, Weitzner

Northeastern University
Silevitch

Oak Ridge National Lab.
Dory, Meier, Mook

Princeton Plasma Physics Lab
Chen, Cheng, Lee, Okuda, Tang, Graydon

Sandia Labs, Albuquerque
Freeman, Humphries, Poukey, Quintenz, Wright

Sandia Labs, Livermore
Marx

Science Applications, Inc.
Drobot, Mankofsky, McBride, Siambis, Smith

Stanford University
Blake, Buneman

University of Arizona
Morse

University of California, Berkeley
Arons, Chen, Chorin, Grisham, Hudson, Keith, Lichtenberg, Lieberman, McKee, Morse, Otani, Thomas, Kim, Lawson, Crystal, Kuhn, Birdsall, Wendt

University of California, Davis
DeGroot, Woo

University of California, Irvine
Rynn

University of California, Los Angeles
Dawson, Decyk, Huff, Lin

University of Iowa
Knorr, Nicholson

University of Maryland
Guillory, Rowland, Winske

University of Pittsburgh
Zabusky

University of Texas
Horton, McMahon, Tajima

University of Washington
Potter

University of Wisconsin
Shohet

Varian Associates
Helmer

Bhabha Research Centre
Aiyer, Gioel

Culham Laboratory
Eastwood, Roberts

Ecole Polytechnique, Lausanne
Hollenstein, Rousset

Ecole Polytechnique, Palaiseau
Adam

Institute Superior Técnico, Lisbon
Brinca

Kyoto University
Abe, Jimbo, Matsumoto

Nagoya University
Kamimura

Max Planck Inst. für Plasmaphysik
Biskamp, Kraft

Osaka University
Mima, Nishihara

Oxford University
Allen

Risó National Labs
Lynov, Pécseli

Tel Aviv University
Cuperman

Tohoku University
Saeki, N. Sato

Universität Bochum
Schamel

Universität Kaiserslautern
Wick

University of Reading
Hockney

University of Tromsó
Trulsen


END
FILMED
8-83
DTIC